CrossMark

The total cross sections of the ^{11}B(α,n)^{14}N and the ^{10}B(α,n)^{13}N reactions between 2 and 6 MeV

R. M. Prior[1] · M. C. Spraker[1] · R. H. France[2] · S. Stave[3,4] · M. W. Ahmed[3,4] ·
H. J. Karwowski[4,5] · J. M. Mueller[3,4] · L. S. Myers[3,4,6] · H. R. Weller[3,4]

© Shanghai Institute of Applied Physics, Chinese Academy of Sciences, Chinese Nuclear Society, Science Press China and Springer Nature Singapore Pte Ltd. 2017

Abstract There is considerable interest in potential aneutronic fusion reactors. One possible reaction is ^{11}B(p,α)2α. However, the emitted alpha particles are energetic enough to generate neutrons by interacting with boron inside the reactor through the ^{11}B(α,n)^{14}N and ^{10}B(α,n)^{13}N reactions. To aid in evaluating neutron production within this potential aneutronic reactor, the total cross sections were measured for the ^{11}B(α,n)^{14}N reaction between 2 and 6 MeV and for the ^{10}B(α,n)^{13}N reaction between 2 and 4.8 MeV. The results are presented and compared with previously reported results.

Keywords Boron · Neutrons · Fusion · Alpha reactions

1 Introduction

For many years, most of the fusion reactors that have been studied use nuclear reactions whose primary product is energetic neutrons. The energy of these neutrons must subsequently be converted into electric power. The large neutron fluxes require significant radiation shielding and also produce activation of the surrounding materials. An alternative is aneutronic fusion in which neutrons carry very little of the released energy. One example of aneutronic fusion uses the ^{11}B(p,α)2α reaction whose final product is three alpha particles [1]. There is a resonance in the ^{11}B(p,α)2α reaction at a proton energy of 0.675 MeV that would be the main producer of the reaction in the proposed fusion reactor [2].

This reaction produces no neutrons, but secondary reactions of the energetic alpha particles may produce neutrons. The ^{11}B(α,n)^{14}N reaction is the most troublesome side reaction in a plasma fusion reactor that uses the reaction ^{11}B(p,α)2α for power production. Even though - means exist to minimize the retention of product alphas inside the fusing plasma, some low-density buildup cannot be avoided. Thus, to most accurately evaluate the reactor material's neutron damage and radioactivation, as well as any biological shielding requirements, it is necessary to have full confidence in the value of the ^{11}B(α,n)^{14}N reaction cross section. Although a very low ^{10}B admixture is anticipated in the boron fuel, an update to the ^{10}B(α,n)^{13}N reaction cross section is also useful.

Fusion alphas are produced with average energies of about 3 MeV with a peaking in the spectrum around 4 MeV. The ^{11}B(α,n)^{14}N reaction has been studied several times in the past in the energy region below 6 MeV [3–10]. There is considerable disagreement between these different data sets, and the coverage of the energy range below 6 MeV is incomplete. The situation is similar for the ^{10}B(α,n)^{13}N reaction [3, 4, 9, 11–13]. The purpose of the present measurement was to obtain the total cross sections

✉ R. M. Prior
richard.prior@ung.edu

[1] University of North Georgia, Dahlonega, GA 30597, USA

[2] Georgia College & State University, Milledgeville, GA 31061, USA

[3] Duke University, Durham, NC 27708, USA

[4] Triangle Universities Nuclear Laboratory, Durham, NC 27708, USA

[5] University of North Carolina, Chapel Hill, NC 27599, USA

[6] Present Address: Bluffton University, Bluffton, OH 45817, USA

in the alpha energy range between 2 and 6 MeV for the ^{11}B target and between 2 and 4.8 MeV for the ^{10}B target.

2 Experimental procedure

The measurement used the INVS Model IV neutron counter [14, 15]. The INVS detector consists of a cylindrical polyethylene body 46.2 cm long and 30.5 cm in outer diameter, and it has an axial cavity 8.9 cm in diameter. The purpose of the polyethylene is to moderate the neutrons. The moderated neutrons are detected by 18 tubular ^{3}He proportional counter tubes (6 atm of ^{3}He) that are embedded in the polyethylene in two concentric rings. Because of the 0.734 MeV Q-value of the ^{3}He$(n,p)^3$H reaction, the signals from the neutrons are much larger than background signals caused by gamma rays and electronic noise. A fixed threshold discriminator effectively discriminates against all signals except those caused by neutrons. Signal processing built into the detector structure produces three TTL output signals: (1) the signals from the inner ring of ^{3}He detectors, (2) the signals from the outer ring of detectors and (3) the logical OR of the signals from both rings of detectors. The INVS detector geometry and operation are discussed in detail in Refs. [14, 15].

The neutron-producing target was located at the center of the 8.9-cm-diameter and 46-cm-long cylindrical cavity on the axis of the polyethylene cylinder. As shown in Ref. [15], the efficiency of this detector can be calculated with the Monte Carlo code MCNPX (using data file ENDF/B-VII.0). The detailed geometry of the detector is included in the calculations. The ground-state Q-values of the reactions were 0.158 MeV for the ^{11}B$(\alpha,n)^{14}$N reaction and 1.059 MeV for the ^{10}B$(a,n)^{13}$N, producing neutrons in this experiment that ranged from 1 to 5.7 MeV in energy. For these neutrons, the INVS counter is very efficient with the calculated total efficiencies for the neutrons in this experiment ranging from 0.51 to 0.18.

The targets consisted of isotopically pure ($\sim$99%) ^{11}B and ^{10}B deposited on 1.3-mm-thick tantalum backings. The targets were produced by ACF [16]. The nominal target thicknesses were 2.25 μg/cm^2 for ^{11}B and 8 μg/cm^2 for ^{10}B. The calculated energy loss of the incident alpha particles in the ^{11}B targets ranged from 3.2 down to 1.5 keV, respectively, for alpha particles from 2 to 6 MeV. For the ^{10}B targets, the energy loss ranged from 10.6 to 3.7 keV. The targets were mounted in a small vacuum chamber that was located at the center of the detector cavity. The alpha particle beam entered along the axis of the counter. The targets were mounted on a disk that could be rotated to alternately expose a ^{11}B target, a ^{10}B target and a blank tantalum disk to the beam. The blank disk was used to measure the neutron background under the same beam conditions as the ^{11}B or ^{10}B measurements. The Triangle Universities Nuclear Laboratory Tandem accelerator was used to produce beams of doubly charged alpha particles with energies from 2.0 to 6.0 MeV in energy steps of 0.10 MeV. Beam currents on target ranged from 30 to 150 nA. The typical counting time per energy was about 10 min to produce statistical precision below 1%. By repeating measurements at several different energies throughout the data taking, it was determined that there was no deterioration of the targets in the experiment.

3 Data reduction for the ^{11}B$(\alpha,n)^{14}$N reaction

The data consisted of counts from the detector obtained for measured beam integrations. Because of the high efficiency of the detector, the statistical precision of all the measurements was well below 1% so that statistical errors were negligible compared with other errors. The background counts were always less than 1% so that background subtraction was not required.

We define the detector efficiency to be the ratio of the number of neutrons actually detected divided by the number of neutrons emitted from the target. This means that the solid angle of the detector array is included in this quantity. The detector efficiency varies with the energy of the neutrons. There is also a small effect due to the anisotropic angular distribution of the neutrons from the target. The measurements and calculations of Arnold et al. [15] indicate that calculating the detector efficiency with the MCNPX code is accurate to within 6%. The MCNPX code was used in this experiment with the specified geometry of the detector and the neutron-producing target located at the center of the detector cavity. The energy and angular distributions of the neutrons were varied, and the efficiency of the detector was calculated for a wide range of these distributions. The geometry of the target structure was not included in the calculations. The only part of the target structure that could significantly attenuate the neutrons reaching the detector is a stepper motor that was used to rotate from one target to another. However, that motor was located in line directly behind the target and could only intercept neutrons that would have escaped from the hole at the end of the detector cavity which was considered in the calculations.

The simplest calculation of the detector efficiency is for an isotropic source of monoenergetic neutrons. This requires running MCNPX for different energies over the range of the energies observed in this experiment. The results of these calculations are shown in Fig. 1.

A more sophisticated calculation includes the neutron energy variation with the angle of emission from the target. In Fig. 2, the angular distribution of emitted neutrons was
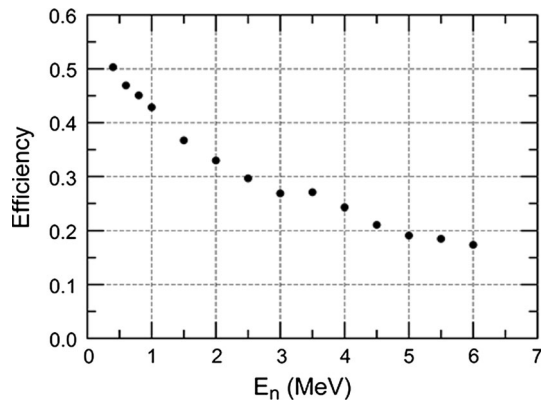
Fig. 1 Calculated efficiency for the INVS detector for isotropic monoenergetic neutron sources located at the center of the detector as a function of neutron energy
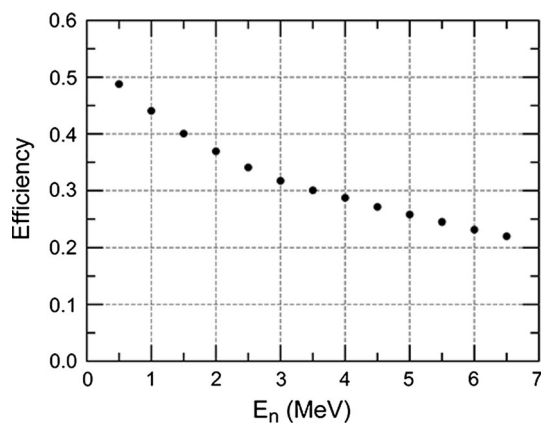

Fig. 2 Calculated efficiency for the INVS detector for isotropic neutron sources located at the center of the detector with energy variation of the neutron energy for the kinematics of the ^{11}B(α,n_0)^{14}N reaction

isotropic, and the neutron energies varied with emission angle as calculated for the kinematics of the ^{11}B(α,n_0)^{14}N reaction for a range of incident alpha particle energies from 0.5 to 6.5 MeV.

An anisotropic angular distribution can affect the efficiency because it weights the neutron energies at some angles more heavily than at other angles. Using the angular distributions measured by Van der Zwan and Geiger [7], MCNPX calculations of efficiency were performed at several energies where the anisotropy of the angular distributions was significant. In most cases, the effects on the efficiency were a few percent or less. At only one point between 5.5 and 6.0 MeV alpha particle energies did the variation exceed 5%, and at most energies it was much less than 5%. Because of the small effects of anisotropy, the efficiency calculations at most energies did not include those effects.

These efficiency calculations were all performed under the assumption of a single neutron energy at each angle, calculated for the ^{11}B(α,n_0)^{14}N reaction. This is valid for

alpha particle energies below 2.94 MeV, the threshold of the ^{11}B(α,n_1)^{14}N reaction. The ^{11}B(α,n_2)^{14}N reaction also begins to contribute at its threshold energy of 5.17 MeV,. The energies of the neutrons emitted in these reactions are lower than the neutrons from the ^{11}B(α,n_0)^{14}N reaction, and thus, the detector has a higher efficiency for them. The data of Van der Zwan and Geiger [7] measured the 0° cross sections for all three of these reactions. Assuming that the 0° cross sections represent the relative intensities of the three reactions, these data can be used to calculate a weighted average efficiency at each alpha particle energy by using the relative strengths of the reactions and the efficiencies corresponding to each neutron group. This correction affects the results for alpha particle energies between 3.5 and 4.5 MeV because of the n_1 neutron group and above 5.5 MeV because of the n_2 neutron group. At all other energies, the corrections were negligible. The uncertainties in this correction process increased the systematic error to 10% in the regions where the corrections were applied between 3.5 and 4.5 MeV and above 5.5 MeV incident alpha particle energies.

The MCNPX efficiency calculations for isotropic neutron sources with kinematic energy variation of the neutron energy were adjusted as described above and then used with the data acquired in the experiment to extract the experimental total cross section. Because of the manufacturer's unknown uncertainty in the ^{11}B target thickness, the cross section was normalized to the total cross-sectional results of Wang et al. [10] at 2.3 and 2.4 MeV. The cross-sectional data of Ref. [12] had a quoted accuracy of 5%. The corrected target thickness was found to be 2.25 ± 0.12 µg/cm^2. The normalization was done to these data because it was judged to be the most precise in this energy region and because the cross section was flat and nonresonant in the 2.3–2.4 MeV region.

3.1 Data reduction for the ^{10}B(α,n)^{13}N reaction

The data for this reaction are complicated by the presence of strong neutron groups that leave the residual ^{13}N nucleus in excited states, producing neutrons of different energies from those which go to the ground state. Since the efficiency of the INVS detector depends upon the energy of the neutrons being detected, a knowledge of the relative intensities of the various neutron groups is necessary in order to determine the detector efficiency.

The ground-state neutron group dominates at alpha energies below 3.5 MeV, making the efficiency calculations relatively straightforward and reliable. At higher energies, the contributions from neutrons to the first excited state (n_1) and especially those to the second and third excited states (n_{23}) become important. This was observed in the INVS detector by a sudden rise in the ratio of the

counting rates of the inner to the outer rings of ^{3}He tubes in the detector at around 3.5 MeV. This is due to the fact that the ratio of the counting rates of the two different detector rings varies as the neutron energy varies [15].

MCNPX calculations of the detector efficiency were performed for energies between 3.5 and 4.8 MeV using the relative yields of neutrons to the various excited states as measured and reported in Ref. [13]. The angular distributions of the outgoing neutrons were assumed to be isotropic. This is an approximation, but an intensive study was performed that showed the effect of this on the final values of the efficiencies was less than a few percent.

The absolute cross section was established by a direct normalization to the results of Van der Zwan and Geiger [13] at $E_\alpha = 2.27$ MeV, since only n_0 neutrons were present at that energy, meaning that the efficiency calculations are very reliable. These authors reported total cross sections at four energies. At 4.57 MeV, they measured the separate cross sections for n_0 (23.6 mb), n_1 (5.9 mb) and $n_2 + n_3$ (48.1 mb) for a total of (78 ± 12) mb. Our present result of 78 ± 8 mb at that energy is in agreement with that result, indicating that our detector efficiencies are reliable even at these higher energies.

The statistical uncertainties in these measurements are negligible since the counting rates were very high. The errors are dominated by the uncertainties in the calculated detector efficiencies. Our best estimate of this uncertainty is 10%, which is the error we have assigned to our final data points.

4 Results

The total cross section of the ^{11}B$(\alpha,n)^{14}$N reaction between 2 and 6 MeV is shown in Fig. 3. Tabular data are included in Table 1. The error bars represent the systematic
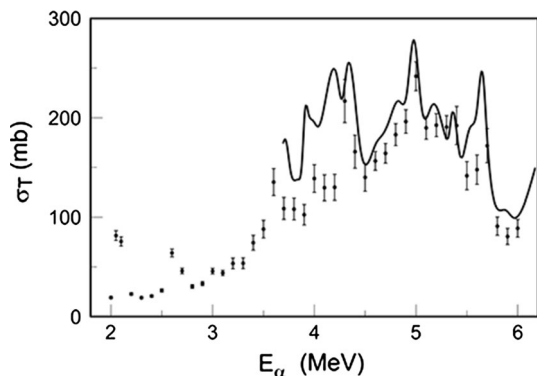

Fig. 3 Total cross section of the ^{11}B$(\alpha,n)^{14}$N reaction. The *error bars* represent the systematic uncertainty associated with the efficiency calculations and do not include the (negligible) statistical uncertainties or the uncertainty in the normalization data. The *solid line* shows the data of Ref. [7]

Table 1 Experimental cross-sectional data for ^{11}B$(\alpha,n)^{14}$N

E_α (MeV)	σ_T (mb)	$\delta\sigma_T$ (mb)
2.0	19.07	1.14
2.1	81.55	4.89
2.1	75.65	4.54
2.2	22.70	1.36
2.3	18.95	1.14
2.4	20.62	1.24
2.5	26.26	1.58
2.6	64.06	3.84
2.7	45.88	2.75
2.8	30.28	1.82
2.9	33.19	1.99
3.0	45.71	2.74
3.1	43.87	2.63
3.2	53.50	5.35
3.3	53.69	5.37
3.4	74.34	7.43
3.5	88.08	8.81
3.6	135.14	13.51
3.7	108.75	10.87
3.8	108.17	10.82
3.9	102.55	10.26
4.0	138.69	13.87
4.1	129.49	12.95
4.2	129.92	12.99
4.3	216.75	21.68
4.4	165.76	16.58
4.5	139.95	14.00
4.6	156.44	9.39
4.7	164.09	9.85
4.8	182.96	10.98
4.9	196.16	11.77
5.0	241.78	14.51
5.1	189.78	11.39
5.2	192.50	11.55
5.3	190.58	11.44
5.4	192.13	19.21
5.5	141.56	14.16
5.6	147.67	14.77
5.7	171.77	17.18
5.8	91.02	9.10
5.9	80.67	8.07
6.0	88.91	8.89

uncertainty due to the efficiency calculations. It does not include the 5% uncertainty of the data in Ref. [10]. In the regions where the ^{11}B$(\alpha,n_0)^{14}$N reaction dominates and no correction were needed, this error was 6% as shown by Arnold et al. [15]. In the correction regions, it was
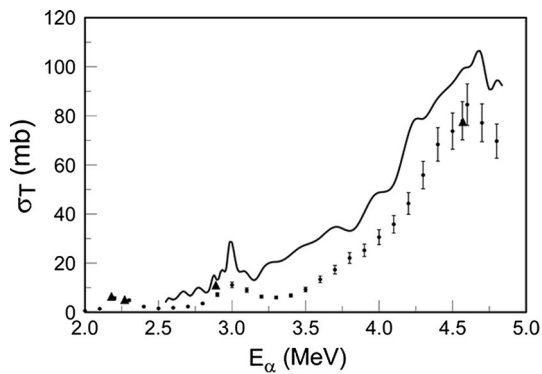
Fig. 4 Total cross section of the ^{10}B(α,n)^{13}N reaction. The *error bars* represent the systematic uncertainty associated with the efficiency calculations and do not include the (negligible) statistical uncertainties or the uncertainty in the normalization data. The *solid line* shows the data of Ref. [12]. The triangle symbols at 2.18, 2.27, 2.89 and 4.57 MeV are from Ref. [13]

Table 2 Experimental cross-sectional data for ^{10}B(α,n)^{13}N

E_α (MeV)	σ_T (mb)	$\delta\sigma_T$ (mb)
2.0	0.57	0.06
2.1	1.37	0.14
2.2	5.71	0.57
2.3	4.86	0.49
2.4	2.28	0.23
2.5	1.53	0.15
2.6	1.80	0.18
2.7	2.30	0.23
2.8	3.55	0.36
2.9	7.08	0.71
2.9	7.20	0.72
3.0	11.10	1.11
3.1	8.98	0.90
3.2	6.33	0.63
3.3	6.00	0.60
3.4	6.79	0.68
3.5	9.23	0.92
3.6	13.36	1.34
3.7	17.30	1.73
3.8	22.07	2.21
3.9	25.23	2.52
4.0	30.59	3.06
4.1	35.83	3.58
4.2	44.29	4.43
4.3	55.87	5.59
4.4	68.35	6.83
4.5	73.76	7.38
4.6	78.00	7.80
4.6	84.58	8.46
4.7	77.17	7.72
4.8	69.69	6.97

increased to 10%. The solid line in Fig. 3 represents the reported total cross-sectional data of Ref. [7].

The total cross section of the ^{10}B(α,n)^{13}N reaction between 2 and 4.8 MeV is shown in Fig. 4. Tabular data are included Table 2. The error bars represent the systematic uncertainty associated with the efficiency calculations and do not include the (negligible) statistical uncertainties or the uncertainty in the normalization data. The solid line shows the data of Ref. [9]. The triangle symbols near 2.18, 2.27, 2.89 and 4.57 MeV are data points from Ref. [13].

5 Comments and conclusions

The measured ^{11}B(α,n)^{14}N cross section agrees generally with the results of Ref. [7] above 3.7 MeV although the present results are 20% or more lower. Our measurements with a thin target were taken in even 0.10 MeV steps so that some of the narrower resonant structures seen by other observers were between the energies at which we measured. The uncertainties in our results are almost entirely due to the uncertainties in the detector efficiency. These were estimated to be 6% at those energies where the n_0 neutrons dominated and 10% in the regions where more than one neutron group made a significant contribution to the yield (between 3.5 and 4.5 MeV and above 5.5 MeV). Statistical errors were insignificant compared with those uncertainties.

The measured ^{10}B(α,n)^{13}N cross section is consistently lower than the cross section of Ref. [12]. The current cross section was normalized to the results of Ref. [14] at 2.27 MeV. The agreement of the data from Ref. [13] at 2.89 and 4.57 MeV with the current data indicates that the energy dependence of both sets of data is very similar.

References

1. N. Rostoker, M.W. Binderbauer, H.J. Monkhorst, Colliding beam fusion reactor. Science **21**, 1419–1422 (1997). doi:10.1126/science.278.5342.1419
2. S. Stave, M.W. Ahmed, R.H. France III et al., Understanding the 11B(p,α)$\alpha\alpha$ reaction at the 0.675 MeV resonance. Phys. Lett. B **696**, 26–29 (2011). doi:10.1016/j.physletb.2010.12.015
3. T.W. Bonner, A.A. Kraus Jr., J.B. Marion et al., Neutrons and gamma rays from the alpha-particle bombardment of ^{9}Be, ^{10}B, ^{11}B, ^{13}C, and ^{18}O. Phys. Rev. **102**, 1348–1354 (1956). doi:10.1103/PhysRev.102.1348
4. E.S. Shire, R.D. Edge, The production of neutrons and protons by the bombardment of boron by low energy alpha-particles. Philos. Mag. **46**, 640–651 (1955). doi:10.1080/14786440608521111
5. J.M. Calvert, N.H. Gale, J.B. Garg et al., Ramavataram, Neutron angular distributions from the reaction ^{11}B(α,n)^{14}N. Nucl. Phys. **31**, 471–477 (1962). doi:10.1016/0029-5582(62)90766-6

6. G.S. Mani, G.C. Dutt, Reaction mechanism for the ^{11}B(α,n)^{14}N reaction. Nucl. Phys. **78**, 613–624 (1966). doi:10.1016/0029-5582(66)90899-6

7. L. van der Zwan, K.W. Geiger, The ^{11}B(α,n)^{14}N cross section for α-energies up to 8 MeV. Nucl. Phys. A **246**, 93–103 (1975). doi:10.1016/0375-9474(75)90565-5

8. M. Niecke, M. Niemeier, R. Weigel et al., Angular distributions of neutron polarization from the ^{14}C(p,n)$_{14}$N and ^{11}B($\alpha,$n)$_{14}$N reactions and the R-matrix analysis of ^{15}N in the excitation-energy range between 11.5 and 12.5 MeV. Nucl. Phys. **A289**, 408–424 (1977). doi:10.1016/0375-9474(77)90043-4

9. J.K. Bair, J. Gomez del Campo, Neutron yields from alpha-particle bombardment. Nucl. Sci. Eng. **71**, 18–28 (1979). doi:10.13182/NSE71-18

10. T.R. Wang, R.B. Vogelaar, R.W. Kavanagh, ^{11}B + α reaction rates and primordial nucleosynthesis. Phys. Rev. C **43**, 883–896 (1991). doi:10.1103/PhysRevC.43.883

11. E.S. Shire, J.R. Wormald, G. Lindsay-Jones et al., Nuclear reactions produced by the bombardment of boron by low energy alpha-particles. Philos. Mag. **44**, 1197–1212 (1953). doi:10.1080/14786441108520385

12. J.H. Gibbons, R. l. Macklin, Total neutron yields from light elements under proton and alpha bombardment. Phys. Rev. **114**, 571–580 (1959). doi:10.1103/PhysRev.114.571

13. L. van der Zwan, K.W. Geiger, The ^{10}B(α,n)^{13}N,^{13}N* cross section for α-energies from 1.0 to 5 MeV. Nucl. Phys. **A216**, 188–198 (1973). doi:10.1016/0375-9474(73)90527-7

14. J.K. Sprinkle Jr, H.O. Menlove, M.C. Miller et al., Los Alamos national lab report no. LA-12496-MS (1993)

15. C.W. Arnold, T.B. Clegg, H.K. Karwowski et al., Characterization of an INVS model IV neutron counter for high precision (γ,n) cross-section measurements. Nucl. Instrum. Methods **A647**, 55–62 (2011). doi:10.1016/j.nima.2011.01.177

16. ACF Metals, Arizona Carbon Foil Company, Tucson, AZ